Electrons in quantum dots: One by one

S. Gustavsson,[1] R. Leturcq,[1] T. Ihn,[1] K. Ensslin,[1,a)] and A. C. Gossard[2]
[1]*Solid State Physics Laboratory, ETH Zurich, 8093 Zurich, Switzerland*
[2]*Department of Materials, University of California, Santa Barbara, California 93106, USA*

(Received 2 September 2008; accepted 16 February 2009; published online 18 June 2009)

A quantum point contact placed close to a quantum dot can be used as a charge detector with time resolution to monitor the charge flow on the level of individual electrons. The current through the quantum point contact may take two possible values corresponding to the situation of an additional electron being on or off the quantum dot. Time traces of such two-level behavior allow to measure the average current, the tunnel rates in and out of the quantum dot, the time-dependent fluctuations of the current (noise), as well as higher-order current correlations. This high-sensitivity method to measure charge flow can also be used to detect time-resolved single-electron interference. © *2009 American Institute of Physics*. [DOI: 10.1063/1.3116227]

I. INTRODUCTION

Electron transport through semiconductor quantum dots can be understood using the concepts of Coulomb blockade as well as sequential and cotunneling through a double barrier system.[1] The current through a quantum dot is limited by the tunnel barriers which can be tuned by gate voltages. For typical transport measurements at temperatures below 100 mK the smallest detectable currents are of the order of 10 fA using typical measurement times of about 1 s per data point. This corresponds to a rate of electrons passing the quantum dot of about 100 kHz. A typical current signal therefore averages over many elementary charges. Noise measurements are a powerful tool to investigate correlations in the current flow which are related to the particular mesoscopic device under investigation. Current correlations are much more difficult to measure than the current itself and require typical current levels of nanoampere if conventional amplifiers and correlation techniques are used. Here we demonstrate that a quantum point contact, or more generally a constriction, placed close to a quantum dot can be used to monitor the current flow in a time-resolved fashion. This gives access to ultrasensitive current measurement down to attoampere, high-resolution measurements of the noise and even higher-order correlations in current flow as well as interference experiments on the level of individual electrons.

II. TIME-RESOLVED ELECTRON TRANSPORT

The sample shown in the left part of Fig. 1 is based on a Ga[Al]As heterostructure with a two-dimensional electron gas (2DEG) 34 nm below the surface. It was fabricated by local oxidation with a scanning force microscope (SFM).[2] The 2DEG is depleted below the oxide lines written on the GaAs surface [bright lines in the top left of Fig. 1] thus defining the quantum dot connected to source and drain contacts as well as the constriction placed above the quantum dot.

As a bias is applied across the quantum dot electrons may flow from source to drain, if a quantum state is in the bias window (see schematic in the lower right part of Fig. 1). For all experiments presented here the electronic temperature is of the order of 100 mK. The thermal broadening in the leads is much smaller than the applied bias. We can therefore safely neglect temperature-activated processes. Because of Coulomb blockade, electrons have to pass sequentially through the quantum dot. Since the quantum dot and the quantum point contact are close to each other they are electrostatically coupled. If an additional electron occupies the quantum dot the potential in the neighboring quantum point contact is affected and the current is reduced. Therefore the quantum point contact can be used as a sensor for the average charge occupation of the quantum dot.[3]

If the tunnel barriers are raised by appropriate gate voltages the transfer rate of the electrons through the dot is reduced and the current becomes too small (less than 10 fA) to be measured by conventional means. However, the charge sensor can still be used to monitor the average charge occupation of the dot. If the current through the quantum point contact is measured as a function of time, it becomes possible to detect the electrons in a time-resolved fashion as they pass the quantum dot.[4,5] A typical time trace of such a situation is displayed in the upper right of Fig. 1. In this case the current in the detector drops from about 6 to about 3.5 nA as an additional electron occupies the quantum dot. The downturns in this trace reflect the situation when an electron enters the dot from the source contact. The upturns correspond to the situation that an electron leaves the dot to the drain contact. Since the bias applied across the dot is much larger than the thermal energy kT we can safely neglect thermal processes which could also reverse the direction of electron transport.

A time trace like the one displayed in the upper right of Fig. 1 contains a lot of information. Counting the downturns (or upturns) as a function of time gives the mean current through the quantum dot. A statistical analysis of the high (low) current states allows to extract the rates for the source (drain) tunneling rates separately.[6] A closer inspection of the count rate also allows to measure noise and higher-order correlations in the current.[6]

For a further analysis we follow the framework devel-

a)Electronic mail: ensslin@phys.ethz.ch.

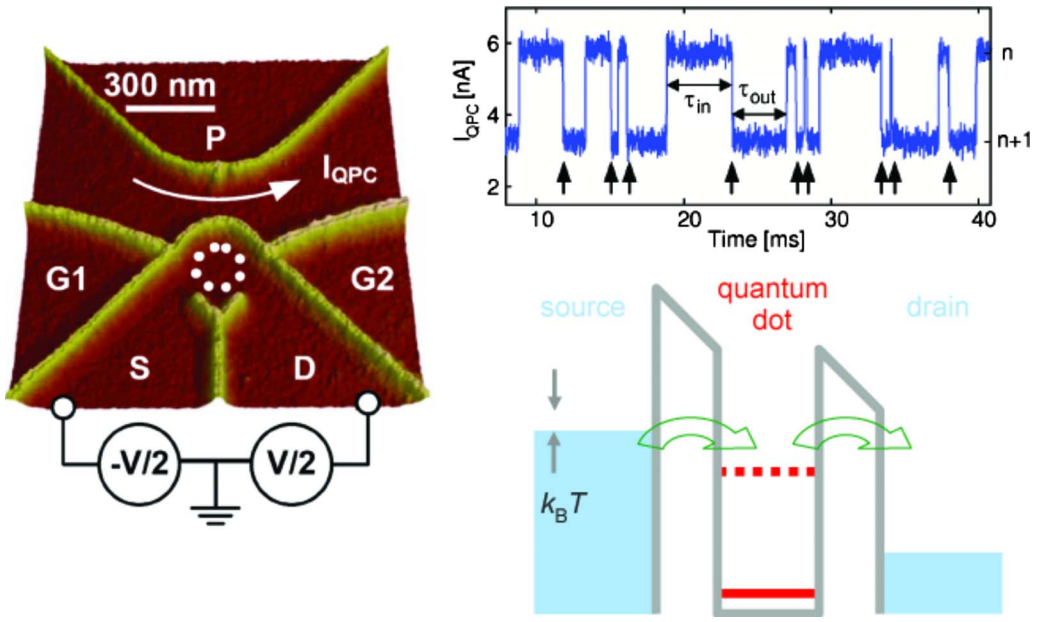

FIG. 1. (Color online) Left: SFM micrograph of the structure. Yellow lines indicate oxide lines written with the atomic force microscope in the surface of the AlGaAs heterostructure. The potential landscape of the electrons residing in the 2DEG 34 nm below the surface is very similar to the potential profile of the oxide lines. Upper right: typical time trace of a quantum point contact signal measured as electrons tunnel into and out of the quantum dot. Lower right: schematic diagram of the energy levels in the quantum dot and the corresponding chemical potentials in the source and drain leads. The applied bias is larger than the thermal smearing kT in the source and drain contacts (adapted from Ref. 6).

oped in the so-called full counting statistics.[7] This method relies on the evaluation of the probability distribution function of the number of electrons transferred through a conductor within a given time period. One starts from a long time trace similar to the one shown in the upper right of Fig. 1. This time trace is divided into smaller intervals of equal length. Then one identifies intervals with a certain number of events and plots the number of intervals found as a function of the number of events in each interval. This procedure results in data such as the one plotted in Fig. 2. The bars arise from the analysis of experimental data and the red line is the calculation.[7] The only adjustable parameter is the scale for the vertical axes, since the number of counts depends on the length of the time trace.

The two distributions shown in Fig. 2 result from data taken on the same sample for slightly different gate voltage settings. While the mean of both distributions is about the same, the width differs by about a factor of 1.5. This means

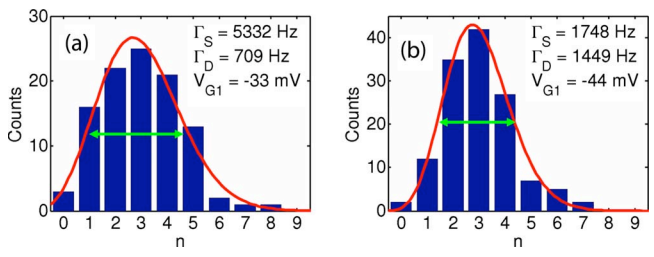

FIG. 2. (Color online) Statistical distribution of the number n of electrons entering the QD during a given time. The two panels, (a) and (b), correspond to two different values of the tunneling rates, obtained for different values of the gate voltage. The time is chosen in order to have the same mean value of number of events for both graphs. We have checked that this choice does not affect the results. The line shows the theoretical distribution. The tunneling rates are determined experimentally, and the theoretical curves are calculated following Ref. 7 (adapted from Ref. 6).

that the mean current flow for the two gate voltage settings is about the same while the noise level differs by about a factor of 2. The numbers indicated in the inset of the two figures show the tunnel rates for source and drain contacts for the two situations. In Fig. 2(a) the two tunnel rates differ by more than a factor of seven. This means that the total current is mostly determined by the thicker tunnel barrier and the situation of tunneling through a single barrier is recovered. This corresponds to classically independent particles following a Poisson distribution which is characterized by a ratio of the current noise with respect to the current, also called the Fano factor, of 1. For the presentation shown in Fig. 2(a) this means that the width of the distribution (i.e., noise) is about the same as the mean of the distribution (i.e., current). In the situation shown in the Fig. 2(b) the tunneling rates for the source and drain barrier are about the same. The tunneling-in rate of an electron is not only determined by the source tunnel barrier, but also by the fact that an electron may not enter an occupied quantum dot because of Coulomb blockade. This additional correlation between successive electrons leads to a reduction in noise, or a Fano factor below one, meaning that the width of the distribution is smaller than its mean.

A more systematic analysis is presented in Fig. 3. The horizontal axis is the asymmetry of the tunnel barriers. For a given gate voltage setting the tunnel barriers can be determined from time traces such as the one shown in Fig. 1. From these time traces the asymmetry of the two barriers can be calculated without any adjustable parameter. The vertical axis in Fig. 3(a) is the Fano factor, i.e., the ratio of the width and the mean of the distribution. In Fig. 3(b) the same data is shown, but this time for the ratio of the third and the first moment of the distribution. The dotted line follows the calculation in Refs. 8 and 9 as indicated by the equations which

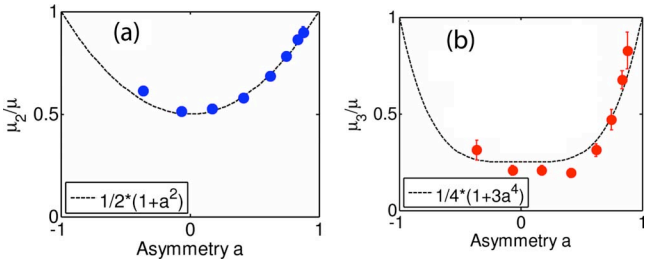

FIG. 3. (Color online) (a) Second and (b) third normalized central moments of the fluctuations of n as a function of the asymmetry of the tunneling rates. The dashed lines are the theoretical predictions. No fitting parameters have been used since the tunneling rates are fully determined experimentally. (adapted from Ref. 6)

are shown in the lower left corners of Figs. 3(a) and 3(b). No adjustable parameters are used. Longer time traces allow for better statistics and the determination of higher-order moments of the distribution.[10] Theory assumes a detector with infinite bandwidth and time traces with infinite length. Both quantities are finite in the experiment but can be measured. The typical bandwidth in our setup is around 30 kHz and is limited by the cabling of the cryostat and the amplifiers. The finite bandwidth and the length of the time traces can be explicitly taken into account for a quantitative comparison of experiment and theory.[11]

III. TIME-RESOLVED DETECTION OF SINGLE ELECTRON INTERFERENCE

The interference of phase-coherent particles is one of the hallmarks of quantum mechanics to demonstrate the wave-particle duality. Usually interference experiments are done with a beam of particles (photons, electrons, atoms, etc.). In order to demonstrate that it is really the wave packet composed of one particle which interferes with itself, it is necessary to make sure that only one particle is in the experimental setup at a given time. For massive particles such an experiment was performed by Tonomura *et al.*[12] who sent electrons one by one through an electron microscope which had a double slit arrangement before the detection screen. A similar experiment in a solid-state environment requires the exquisite control of the relevant quantum mechanical degrees of freedom. A screen with spatial resolution is difficult to realize in a mesoscopic device. Therefore we use an Aharonov–Bohm-type setup where the relative phase of the two interfering trajectories can be tuned by a magnetic flux.

The sample is shown in Fig. 4(a). Electrons enter from the source contact (S) into the double dot (1,2) and then leave to the drain contact (D). The two dots 1 and 2 are coupled by two tunnel barriers. The oxide dot in the center between the two dots makes sure that electron going from dot 1 to dot 2 have two possible paths which is required for an interference experiment. The schematic in Fig. 4(d) indicates the tunnel rates extracted from experiments not shown here.[13] With our detector bandwidth of 30 kHz we can measure the tunneling rates between source and dot 1 and between dot 2 and drain. The tunneling rate between the two dots is of the order of gigahertz and too fast to be detected by our setup. Three typical time traces are shown in Fig. 4(b).

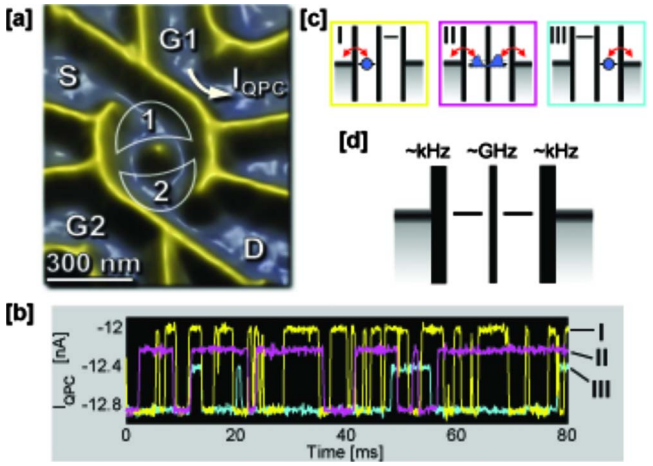

FIG. 4. (Color online) (a) Double quantum dot used in the experiment. Yellow lines are written with a scanning force microscope on top of a semiconductor heterostructure and represent the potential landscape for the electrons. The QDs (marked by 1 and 2) are connected by two separate arms, allowing partial waves taking different paths to interfere. The current in the nearby (I_{QPC}) is used to monitor the electron population in the system. (b) Time traces for three different arrangements of the dot levels and the Fermi levels in source and drain. (c) Schematic of the level arrangement with color code numbered I, II, and III related to the three time traces in (b). (d) Schematic of the tunnel rates connecting the double dot to source and drain (kilohertz) as well as the tunnel rate between the two dots (gigahertz).

They are color-coded with respect to the schematics presented in Fig. 4(c) which indicate the relevant arrangement of the involved energy levels tuned by suitable gate voltages. These time traces allow to extract tunnel rates as well as higher-order correlations in the tunneling processes as described before for a single quantum dot. In addition the amplitude of the time traces indicates the location of the electron distribution which is monitored. The blue time trace has the smallest amplitude because the electrons being detected reside in quantum dot 2 which is farthest away from the charge detector. The yellow time trace, on the other hand, has the highest amplitude, since it reflects tunneling events between the source contact and dot 1, which is closest to the detector. The time trace shown in magenta is for the situation where tunneling events between the two dots are possible since the levels are aligned. The tunneling events occur on time scales (gigahertz) much faster than what can be resolved by the detector (kilohertz). Nevertheless, the amplitude of the magenta-colored time trace is between the amplitudes of the blue and the yellow time traces since in the intermediate case the monitored events are related to electrons residing in a state which extends into both quantum dots. The events which are related to electron tunneling events between either source or drain and the double dot do not depend on the interference of the two partial waves around the center of the dot. The tunneling events between the two dots, which do contain the interference information, are too fast and not accessible for our detector due to bandwidth limitations. It will be an interesting experimental problem in the future, whether and how a detector with a higher bandwidth may allow for which path detection and therefore lead to a reduction in the amplitude of the phase coherent signal.

In order to overcome our experimental bandwidth limi-

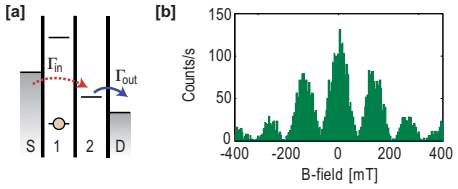

FIG. 5. (Color online) (a) Energy level configuration of the double quantum dot. Electron transport from source to QD2 is possible by means of cotunneling. (b) Number of electrons arriving at QD2 within a fixed period, measured as a function of magnetic field. The count rate shows an oscillatory pattern with a visibility higher than 90%. (adapted from Ref. 16)

tations the sample has been tuned to a special regime which is indicated in Fig. 5(a). In this configuration the tunneling-in process brings an electron from the source contact via cotunneling through dot 1 directly into dot 2. The tunneling-out process is a standard sequential tunneling process from dot 2 into the drain contact. The rate of the tunneling-in process is limited by the tunnel barrier between source and dot 1 and therefore slow and measurable by our detector. At the same time this process contains two possible trajectories around the center antidot and therefore the relative phase between these partial waves can be tuned by a perpendicular magnetic field.

Figure 5(b) shows the experimentally measured count rate versus magnetic field applied perpendicular to the sample plane. A clear *B*-periodic pattern arises whose periodicity agrees with an estimate based on the characteristic enclosed area of the trajectories. In contrast to most Aharonov–Bohm experiments performed on open geometries (e.g., Refs. 14 and 15) the amplitude of the oscillatory signal is more than 90% of the total signal. For electrons cotunneling through dot 1 there is only a discrete state and no electrons from a surrounding Fermi sea for phase-breaking scattering processes are available. A more detailed analysis of the relevant time traces allows to determine the tunneling-in and tunneling-out rates as well as the noise and higher correlations.[16] This way one can show that only the tunneling-in rates containing the two partial waves around the antidot are periodic in magnetic field, while the tunneling-out rates are independent of magnetic field. Upon reversal of the bias direction across the double dot the magnetic field dependence is exchanged between the two rates.[16]

IV. CONCLUSIONS

Time-resolved charge detection is a well-developed tool also used for the investigation of single-spin dynamics.[17] We have demonstrated that this method is versatile to investigate weakly coupled quantum dots where the tunneling currents are too small to be measured by conventional means. In addition ultralow noise levels can be measured with noise powers about six orders of magnitude smaller than accessible by standard measurement techniques. With improved statistics also higher-order correlations in the electron flow can be measured. The general detection technique of a constriction which is capacitively coupled to a nearby quantum dot has been extended to InAs nanowire quantum dots,[18] graphene nanostructures,[19] and single hole devices realized on AlGaAs heterostructures.[20] Also the backaction of a highly biased quantum point contact measuring the charge occupancy of a nearby double dot has been investigated.[21] Future experiments will work toward increased bandwidth in order to measure faster processes and in the end reach the regime of real quantum detection.

ACKNOWLEDGMENTS

Financial support from the Swiss Science Foundation (Schweizerischer Nationalfonds) is gratefully acknowledged.

[1] L. P. Kouwenhoven, C. M. Marcus, P. L. McEuen, S. Tarucha, R. M. Westervelt, and N. S. Wingreen, in *Mesoscopic Electron Transport*, edited by L. P. Kouwenhoven, G. Schön, and L. L. Sohn (Springer, New York, 1997), Vol. 345, pp. 105–214.
[2] A. Fuhrer, A. Dorn, S. Lüscher, T. Heinzel, K. Ensslin, W. Wegscheider, and M. Bichler, Superlattices Microstruct. **31**, 19 (2002).
[3] M. Field, C. G. Smith, M. Pepper, D. A. Ritchie, J. E. F. Frost, G. A. C. Jones, and D. G. Hasko, Phys. Rev. Lett. **70**, 1311 (1993).
[4] R. Schleser, E. Ruh, T. Ihn, K. Ensslin, D. C. Driscoll, and A. C. Gossard, Appl. Phys. Lett. **85**, 2005 (2004).
[5] L. M. K. Vandersypen, J. M. Elzerman, R. N. Schouten, L. H. Willems van Beveren, R. Hanson, and L. P. Kouwenhoven, Appl. Phys. Lett. **85**, 4394 (2004).
[6] S. Gustavsson, R. Leturcq, B. Simovic, R. Schleser, T. Ihn, P. Studerus, K. Ensslin, D. C. Driscoll, and A. C. Gossard, Phys. Rev. Lett. **96**, 076605 (2006).
[7] L. S. Levitov, H. Lee, and G. B. Lesovik, J. Math. Phys. **37**, 4845 (1996).
[8] S. Hershfield, J. H. Davies, P. Hyldgaard, C. J. Stanton, and J. W. Wilkins, Phys. Rev. B **47**, 1967 (1993).
[9] D. A. Bagrets and Y. V. Nazarov, Phys. Rev. B **67**, 085316 (2003).
[10] S. Gustavsson, R. Leturcq, T. Ihn, K. Ensslin, M. Reinwald, and W. Wegscheider, Phys. Rev. B **75**, 075314 (2007).
[11] S. Gustavsson, R. Leturcq, B. Simovic, R. Schleser, P. Studerus, T. Ihn, K. Ensslin, D. C. Driscoll, and A. C. Gossard, Phys. Rev. B **74**, 195305 (2006).
[12] A. Tonomura, J. Endo, T. Matsuda, T. Kawasaki, and H. Ezawa, Am. J. Phys. **57**, 117 (1989).
[13] S. Gustavsson, M. Studer, R. Leturcq, T. Ihn, K. Ensslin, D. C. Driscoll, and A. C. Gossard, Phys. Rev. B **78**, 155309 (2008).
[14] A. Yacoby, M. Heiblum, D. Mahalu, and H. Shtrikman, Phys. Rev. Lett. **74**, 4047 (1995).
[15] M. Sigrist, T. Ihn, K. Ensslin, M. Reinwald, and W. Wegscheider, Phys. Rev. Lett. **98**, 036805 (2007).
[16] S. Gustavsson, R. Leturcq, M. Studer, T. Ihn, K. Ensslin, D. C. Driscoll, and A. C. Gossard, Nano Lett. **8**, 2547 (2008).
[17] J. M. Elzerman, R. Hanson, L. H. Willems van Beveren, B. Witkamp, L. M. K. Vandersypen, and L. P. Kouwenhoven, Nature (London) **430**, 431 (2004).
[18] I. Shorubalko, R. Leturcq, A. Pfund, D. Tyndall, R. Krischek, S. Schön, and K. Ensslin, Nano Lett. **8**, 382 (2008).
[19] J. Güttinger, C. Stampfer, S. Hellmüller, F. Molitor, T. Ihn, and K. Ensslin, Appl. Phys. Lett. **93**, 212102 (2008).
[20] Y. Komijani, M. Csontos, T. Ihn, K. Ensslin, D. Reuter, and A. D. Wieck (unpublished).
[21] S. Gustavsson, M. Studer, R. Leturcq, T. Ihn, K. Ensslin, D. C. Driscoll, and A. C. Gossard, Phys. Rev. Lett. **99**, 206804 (2007).